Applied Computing and Geosciences 23 (2024) 100177

Contents lists available at ScienceDirect

Applied Computing and Geosciences

journal homepage: www.sciencedirect.com/journal/applied-computing-and-geosciences

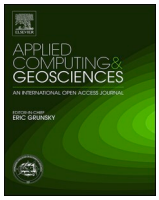

Using multiple-point geostatistics for geomodeling of a vein-type gold deposit

Aida Zhexenbayeva [a], Nasser Madani [a,*], Philippe Renard [b], Julien Straubhaar [b]

[a] School of Mining and Geosciences, Nazarbayev University, Astana, Kazakhstan
[b] Stochastic Hydrogeology Group, University of Neuchâtel, Neuchâtel, Switzerland

ARTICLE INFO

Keywords:
Cascade modeling
Multiple-point statistics
Direct sampling
Training image
Gold deposit
Resource modeling
Sequential Gaussian simulation
Probabilistic approach

ABSTRACT

Geostatistical cascade modeling of Mineral Resources is challenging in vein-type gold deposits. The narrow shape and long-range features of these auriferous veins, coupled with the paucity of drill-hole data, can complicate the modeling process and make the use of two-point geostatistical algorithms impractical. Instead, multiple-point geostatistics techniques can be a suitable alternative. However, the most challenging part in implementing the MPS is to use a suitable training data set or training image (TI). In this paper, we suggest using the radial basis function algorithm to build a training image and the DeeSse algorithm, one of the multiple-point statistics (MPS) methods, to model two long-range veins in a gold deposit. It is demonstrated that DeeSse can replicate long-range vein features better than plurigaussian simulation techniques when there is a lack of conditioning data. This is shown by several validation processes, such as comparing simulation results with an interpretive geological block model and replicating geological proportions.

1. Introduction

A Mineral Resource estimation model is needed for mining project planning (Rossi and Deutsch 2014). Cascade resource modeling allows one to first create the geological domains and then to model the grades of the mineral of interest in each domain separately (Alabert and Massonnat, 1990; Roldão et al., 2012; Boucher and Dimitrakopoulos, 2012; Jones et al., 2013). The domains are often selected based on geological interpretation, including lithology, rock types, grade thresholds, and the assumption that the continuous variables are homogeneous and stationary within the appropriate domain (Rossi and Deutsch 2014). The estimation of grades within each domain can be implemented using different interpolation algorithms. Considerable challenges can be encountered when modeling the geological domains. Although deterministic modeling of geological domains can be straightforward, such a model does not reflect uncertainty across geological domain boundaries, particularly in the areas where the borehole dataset is scarce. In contrast, geostatistical simulation enhances the geological interpretation and measures the uncertainty in the location of the domain boundaries by creating several numerical outputs or realizations of the geological domains. However, using these techniques in modeling long-range and narrow geological features (such as gold veins) is challenging. Two-point geostatistics, such as the sequential indicator simulation (Journel and Gómez-Hernández, 1993) and plurigaussian simulations (Armstrong et al., 2011; Madani, 2021), can be used to stochastically model the geological domains, but they may fail to adequately model the long-range features of geological domains (Abulkhair and Madani, 2022). Instead, multiple-point statistics (MPS) (Guardiano and Srivastava, 1993a,b; Strebelle, 2002) have demonstrated their relevance for simulating heterogeneous structures and long-range geological features (Mariethoz and Caers, 2014). Several techniques based on multiple-point statistics have emerged in recent decades, such as single normal equation simulation (SNESIM) (Strebelle, 2002) or filter-based simulation (FILTERSIM) (Zhang et al., 2006), which enable the replication of increasingly complex geometries and spatial patterns. This work focuses on using the Direct Sampling (DeeSse) (Mariethoz et al., 2010) approach, one of the latest MPS-developed algorithms, which relies on a training image (TI) similar to other MPS-based algorithms. The benefit of DeeSse is that it scans the TI using a distance function rather than constructing a catalog of patterns, which is common in other MPS algorithms. This approach significantly speeds up the simulation and reduces memory usage. The most challenging step in MPS might be the choice of a reliable TI (Emery and Lantuejoul, 2014; Boisvert et al., 2007; Mariethoz and Caers, 2014;

* Corresponding author.
E-mail address: nasser.madani@nu.edu.kz (N. Madani).

https://doi.org/10.1016/j.acags.2024.100177
Received 21 June 2023; Received in revised form 28 June 2024; Accepted 11 July 2024
Available online 17 July 2024

Dubrule, 2017). One solution to this difficulty is to employ explicit or implicit geological models to create such a dataset. Explicit modeling combines hand contouring and wireframing to connect polygons from 2D cross-sections and mold the ore body geometry into a 3D model (Vistelius, 1989; Houlding, 1994; Mallet, 1992, 2002). In the mining industry, it is typical to utilize explicit models like wireframes as TI in MPS workflow (Goodfellow et al., 2012a,b; Boucher et al., 2014; Robles-Stefoni and Dimitrakopoulos, 2016; Rezaee et al., 2014; Quigley et al., 2018; Paithankar and Chatterjee, 2018). However, explicit modeling itself is labor-intensive and often subjective to the geologist's perspective (Silva and Deutsch, 2014, 2015). In contrast, implicit modeling techniques such as indicator kriging (Deutsch and Journel, 1998), Radial Basis Function (RBF) (Franke, 1982), and Support Vector Classification (SVC) (Smirnoff et al., 2008; Hardy, 1971) automate geological boundary construction, reducing manual digitization time. The latter, RBF algorithm, is popular among geo-modelers and is available through several commercial software programs.

Silva and Deutsch (2014, 2015) provided an alternative to integrate two TIs in the MPS algorithm instead of using only one unique TI, leading to the capture of both short and large-scale geological features in the simulation results. In this workflow, one image is deduced from an implicit geological model and another image is derived from Sequential Indicator Simulation. The former and latter represent the large-scale and the short-scale geological features, respectively. Although this algorithm appears to be efficient in reproducing the expected geological outputs, it is slow in performance due to the involvement of the Single Normal Equation Simulation (SNESIM) algorithm (Strebelle, 2002) as the main engine in this stochastic technique. This is because the SNESIM algorithm is insufficient for modeling a large number of cells (Tahmasebi, 2018).

In this work, DeeSse is used to model four geological domains in a gold deposit, where the veins showed a long-range geological feature. The TI is created using the RBF algorithm. Then, following the cascade paradigm, sequential Gaussian simulation (SGS) (Goovaerts, 1997) is used to model the gold in each domain independently and then to derive the final predictive model of the entire gold deposit. The results are then compared with plurigaussian simulations, deterministic cascade modeling, and a case where the influence of geological domains is neglected.

This paper introduces a novel method to quantify the uncertainty of geodomains. Implicit geological modeling with Radial Basis Functions often falls short in capturing the full range of uncertainties due to its deterministic nature. In contrast, the proposed approach employs MPS to provide a representation of uncertainty. This approach is particularly effective for stochastically modeling vein-type deposits, which are characterized by their irregular and complex structures. By using the proposed method, it is possible to generate stochastic realizations that better reflect the inherent variability and complexity of these deposits. The stochastic realizations are designed to be compatible with the implicit deterministic models of geodomains, thereby bridging the gap between deterministic and probabilistic modeling approaches. By integrating this uncertainty quantification method with existing geological modeling frameworks, the approach enhances the ability to predict and manage geological uncertainties. This has significant implications for resource estimation, risk assessment, and decision-making in the field of geological exploration and mining.

2. Methodology

2.1. Cascade modeling

Cascade resource modeling (Alabert and Massonnat, 1990; Roldão et al., 2012; Boucher and Dimitrakopoulos, 2012; Jones et al., 2013) is a popular method for evaluating ore bodies in various types of deposits. This method needs a deterministic model of geological domains and a model of grade estimation for each domain separately. However, deterministic models do not reflect associated geological uncertainty, which can be detrimental to the final grade estimate model. Therefore, it is recommended to use stochastic models of geological domains for resource estimation. These methods are based on simulation approaches that offer a variety of different scenarios, reflecting the equally plausible spatial distribution of the geo-domains rather than a singular geo-domain layout. Incorporating geological control into Mineral Resource evaluation can be facilitated by utilizing probability maps. One alternative for using the probabilistic description of geological domains in estimating the final grade is to use a weighting equation proposed by Emery and Gonzalez (2007). In this technique, the estimated model is created by multiplying the expected grades for each lithological domain by the likelihood/probability of occurrence of that domain in each block separately. This method takes into account the continuity of the ore grades associated with each lithological domain as well as the uncertainty in the spatial layout of these domains within the deposit (Emery and Gonz'alez, 2007):

$$\text{Final predictive grade} = \sum_{k=1}^{n} \text{Probability}\left(k^{th}\ \text{domain}\right) * \text{Predictive grade}\left(k^{th}\ \text{domain}\right) \quad (1)$$

2.2. Modeling of geological domains

To build the probabilistic model of geological domains as required in Eq. (1), there are several geostatistical approaches. Among others, MPS has demonstrated its relevance for modeling curvilinear and long-range patterns of geological domains in comparison to the conventional variogram-based geostatistical approach (Mariethoz and Caers, 2014). To learn about spatial variability, MPS-based techniques employ a conceptual training data set (TI) rather than two-point statistical functions such as the variogram (Mariethoz and Caers, 2014). The TI can contain multiple collocated variables, situated in space or time, or be limited to a single variable and spatial coordinates (Mariethoz and Caers, 2014). The TI is a key component of all the MPS methods because it represents complex geological features of geological domains.

2.2.1. Multiple-point statistics (a brief review)

The rationale behind the MPS-based approaches is to derive spatial variability information from a conceptual training image (TI), rather than from a covariance function commonly used in two-point geostatistics (Mariethoz and Caers, 2014). Compared to variogram-based algorithms, the main advantage of MPS is its ability to model multiple-point relationships and complex curvilinear patterns that exist in geological settings (Boisvert et al., 2007). Moreover, MPS can analyze and reproduce higher-order statistics obtained from the TI (Boisvert, 2010). This implies that the quality of simulated realizations depends significantly on the quality of the TI, making the construction of TI an extremely important process. Based on numerous examples of MPS performance in modeling curvilinear geological domains, both under-informed and over-informed cases are well-suited for MPS, whereas covariance matrices struggle with such datasets (Mariethoz, 2018). Several authors have analyzed MPS and compared it to variogram-based methods, either by reviewing available algorithms or by applying statistical validation techniques (Boisvert, 2010; De Iaco and Maggio, 2011; Tan et al., 2014; Tahmasebi, 2018; Madani et al., 2019). Apart from applications in petroleum and hydrogeology, MPS has proved applicable in the mining industry as well, particularly for modeling slate deposits (Bastante et al., 2008) and dykes in copper deposits (Rezaee et al., 2014).

Several alternatives to MPS-based algorithms have emerged since Guardiano & Srivastava's initial implementation in 1993, known as extended normal equation simulation (ENESIM). This advancement has seen the introduction of many more sophisticated algorithms. The incorporation of a search tree into ENESIM addresses the CPU time

limitation inherent in single normal equation simulation (SNESIM) (Strebelle, 2002). Additionally, similar algorithms have been developed to simulate patterns rather than pixels, such as filter-based simulation (FILTERSIM) (Zhang et al., 2006) and simulation of patterns (SIMPAT) (Arpat and Caers, 2007). Other alternatives to MPS algorithms include simulated annealing (SA) (Deutsch, 1992), Markov random field (MRF) (Toftaker and Tjelmeland, 2013) methodologies, and the list approach (IMPALA) developed by Straubhaar et al. (2011). Recently, the application of machine learning in the MPS framework has become a focus of various research groups (Avalos and Ortiz, 2020; Bai and Tahmasebi, 2020). Another notable alternative is DeeSSe (Mariethoz et al., 2010), extensively explained in the following sections.

2.2.2. Building training image (TI)

To implement MPS-based algorithms, a training image (TI) needs to be created. There are several methods to develop a TI, including a conceptual geological model, physical principles, geostatistical algorithms, regular statistics, and occasionally empirical methods (Mariethoz and Caers, 2014). Other approaches involve using 2D images of outcrops or aerial photographs (Anderson et al., 1999; Bayer et al., 2011), gridded geological models of deposits with similar geology (Pyrcz et al., 2008), and conceptual models generated using Boolean methods such as object-based (Deutsch and Wang, 1996) and process-based techniques (Pyrcz et al., 2009).

In the mining industry, it is a common practice to use an interpretive geological block model to create the TI (Goodfellow et al., 2012a,b; Boucher et al., 2014; Robles-Stefoni and Dimitrakopoulos, 2016; Quigley et al., 2018; Paithankar and Chatterjee, 2018). These models are typically derived from geological interpretations or interpolated models based on exploration borehole samples available from the deposit.

In this study, we propose to build the TI using the Radial Basis Function (RBF) (Franke, 1982) available in several software programs. The benefit of employing RBF is that it is a fast and automated technique (Seequent, 2022).

This method utilizes the borehole dataset together with geological knowledge to delineate the geodomains in the TI. This approach offers several advantages:

A) Borehole data naturally preserves the geological characteristics in the subsurface. Creating the training image using borehole data ensures that the model accurately represents the geological features observed in the field.
B) The training image is created from drillhole data, accurately depicting the spatial distribution of lithological units, mineralization, and other geological properties recorded in the boreholes.
C) Borehole data frequently provide detailed information on specific subsurface areas. Using this data to generate the training image enables the capture of localized geological variations that may not be adequately represented in regional geological models.
D) Images created from borehole data for training purposes typically exhibit greater geological accuracy than synthetic or conceptual models. This can lead to more precise geological simulations and predictions.

Therefore, in this study, we created TI and used this as an interpretive geological block model for this deposit, upon which further comparative analyses can be based.

2.2.3. Direct sampling approach (DeeSse)

Once the training image is constructed, various MPS algorithms can be employed to conditionally simulate the geological domains at target blocks. Among these algorithms, the DeeSse algorithm (Mariethoz et al., 2010; Straubhaar and Renard, 2021) stands out as a pixel-based MPS technique that utilizes a distance function during the scanning of the TI. This approach is efficient and bypasses the necessity for a conditional cumulative probability distribution function (cpdf) at each step because it directly samples the TI. Consequently, there is no need to store scanning results in a database. The DeeSse algorithm initially assigns each conditioning datum (e.g., borehole data) to the nearest node in the simulation grid. If multiple conditioning data are available for assignment to the same grid node, the closest one is placed to the center of the node (Mariethoz et al., 2010). This strategy helps ensure that the simulated model closely matches the known data points, leading to a more accurate representation of the geological domains in the area. In essence, it assists in producing realistic simulation outcomes that reflect the known spatial patterns and characteristics present in the conditioning data. Then, The DeeSse algorithm uses conditioning data from the simulation grid as data events, samples the TI, and proceeds to the next node following MPS principles. The first parameter of DeeSse is the maximum number n of nodes or conditional data considered in the neighborhood of the node being simulated. The method terminates sampling when it has scanned up to a maximum fraction f of the TI, provided no data events have computed distances below the prescribed acceptance threshold t. The algorithm efficiently scans the target image in an optimum manner to swiftly move to different locations and effectively cover the image, reducing the amount of iterations required during the sampling process. To achieve this, the algorithm selects the node within the TI where the data event around this node has the smallest Euclidean distance from the data event around the simulated location in the simulation grid. In simpler terms, the algorithm chooses the node within the TI that closely matches the conditioning data on the simulation grid, aiming to faithfully reproduce the observed patterns in the TI.

3. Mineral grade modeling

To obtain the predictive model of grades as required in Eq. (1), realizations produced by sequential Gaussian simulation (SGS) (Goovaerts, 1997) can be used. Implementing SGS involves first forward-transforming all continuous values (grades) to a normal distribution, and then back-transforming the simulated results to the raw distribution. To simulate the variable at a specific location, a random value is sampled from the probability distribution and added to the conditioning dataset. The algorithm then proceeds to the next node along the entire random path through the grid. The covariance or variogram function is essential to characterize the spatial continuity of the mineral grade. This is achieved by conducting a variogram analysis on the normal scores of the mineral grade, followed by fitting an appropriate model to the obtained results. The simulation results, comprising an ensemble of realizations, are then averaged to support the predictive model in Eq. (1).

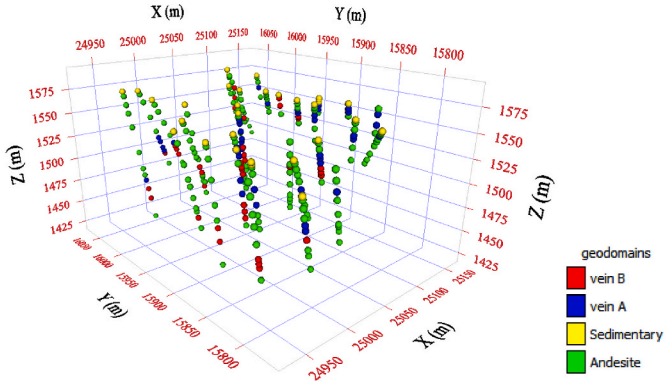

Fig. 1. Isoclinal view of the conditioning borehole dataset. The spheres represent centroids of the intervals logged for lithology.

3.1. Case study – gold deposit

For the actual case study in this research, a borehole dataset (Fig. 1) from a vein-type gold deposit was utilized. The drilling campaign consists of 56 drill-holes covering four geo-domains: sedimentary, andesite and veins A and B. The dataset includes a continuous variable - gold grade, measured in part per million (ppm) (Fig. 2), along with geographic coordinates. Due to confidentiality concerns, the name and location of this gold deposit cannot be disclosed. The veins and host rocks in this deposit are characterized as the ore domains (veins A and B) and waste domains (sedimentary and andesite), respectively. The spatial variability of gold grade is significantly influenced by the studied lithological domains.

3.2. Building training image

The first step in our proposed approach is to create a training image to serve as input for the MPS algorithm. To accomplish this, geo-domains over the borehole samples were targeted for implicit 3D modeling in this deposit using RBF in Leapfrog 2021.2 software package (Seequent, 2022). Initially, we focused on the surface interaction between sedimentary and andesite domains. This involved positioning the sedimentary layer atop the andesite, ensuring contact between them. For the veins, the surface contacts were determined under the assumption of the intrusion concept.

After creating the geological model in this software, the deposit was discretized into 25,530 blocks of dimensions 10 m X 10 m X 10 m along the X, Y, and Z axes, respectively. This solid block model was exported and used as the training image. This model can also be considered as an interpretive geological block model for this deposit. Fig. 3 illustrates the resulting block model of the training image.

3.3. Geostatistical simulations of veins

Geostatistical simulation algorithms are utilized to create an uncertainty model by generating multiple sets of possible values distributed across the analyzed area. These sets of values, known as realizations, are crucial for obtaining a reliable assessment of joint uncertainty (Journel and Huijbregts, 1978). For this particular investigation, 100 realizations of geo-domains were generated to achieve this goal. Stochastic modeling of gold veins was conducted using the DeeSse algorithm in the ISATIS.neo program (Geovariances, 2024). The training image created by Leapfrog was employed for this purpose. To maintain reasonable CPU time, the maximum scan fraction f was set to 0.5, with a maximum of 36 nodes n in the neighborhood. This means only half of the TI can be scanned to locate the node with the shortest similarity distance. The acceptance threshold t was set to 0.02. This aligns with the recommendation by Meerschman et al. (2013), advocating for minimizing this value to effectively replicate geological domains with long-range connectivity. The resulting realizations demonstrate that the structure of gold veins appearing in the TI was accurately replicated by DeeSse as shown in Fig. 4.

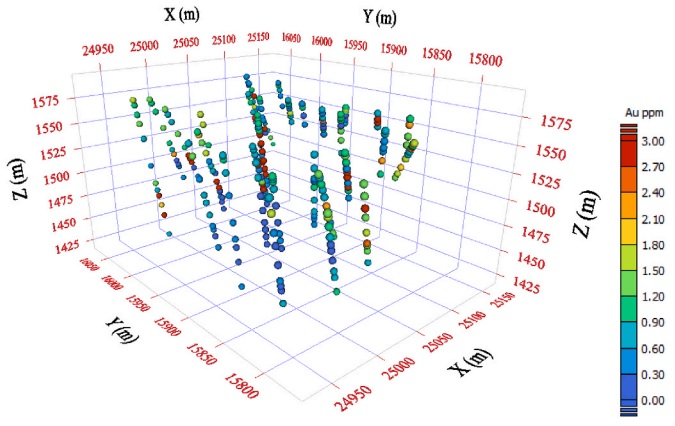

Fig. 2. Isoclinal view of the conditioning borehole dataset. The spheres represent centroids of the intervals logged for gold grade.

The results are then compared with plurigaussian simulation (Armstrong et al., 2011; Madani 2021), a two-point stochastic technique for spatial modeling of categorical variables. A significant feature of this technique is that domain experts can identify and impose the contact relationship between the categories using a flag. To establish plurigaussian models, it is necessary to first identify the contact relationships among geological domains, which can be inferred from borehole data. However, the density of data is sometimes insufficient to establish relationships between geological domains, requiring expert knowledge of the deposit, such as an interpretive geological model, to infer these contact relationships. Therefore, in this study, the model created in Leapfrog (Fig. 3) serves as an interpretive geological block model for this algorithm. As depicted, sedimentary rock contacts both andesite and vein A, while vein B only contacts andesite and vein A. This indicates that sedimentary rock and vein B do not contact each other. This contact relationship, known as flag (Armstrong et al., 2011; Madani, 2021), is illustrated in Fig. 5a. Consequently, two Gaussian random fields (GRF) are considered. The first GRF controls both groups of geological domains, specifically the sedimentary-andesite and veins A and B, while the second GRF model distinguishes between the two veins and also between sedimentary and andesite.

The multidirectional variogram was calculated using borehole data, but due to insufficient data, no clear structure could be deduced from experimental variograms in different directions. Therefore, it was decided to investigate variography using the interpretive geological block model (TI in Fig. 3). For the first GRF, this approach demonstrated better structures with a long-range variogram along the northing direction and comparatively shorter variogram ranges along the east and the vertical directions. In contrast, the second GRF displayed different spatial continuity, showing a long-range variogram structure along the north and east directions and a short-range variogram structure along the vertical direction.

Once the flag and variograms are determined, the next step involves implementing plurigaussian simulations. For this purpose, several alternatives are considered. The first alternative involves a plurigaussian simulation model with a global proportion (GP) of geological domains. This means that the truncation rule is based on the global statistics of the relative frequency (proportion) of geological domains. The global proportions in this alternative are calculated using the interpretive geological block model. The proportions represent the declustered proportions (Madani and Emery, 2015). Proportions of geological domains for sedimentary, andesite, vein A and vein B are 12.62%, 80.69%, 1.69%, and 5.00%, respectively. Andesite dominates the deposit, while Vein A represents the lowest proportion, which poses challenges for the modeling process. The second alternative is to use a vertical proportion curve (VPC) (Armstrong et al., 2011). This curve displays the proportion of each geological domain at each elevation and is highly valuable for modelers because it illustrates the original distribution of the geological domains.

Fig. 5b depicts the computed VPC for this deposit. As observed, sedimentary dominates near the surface, while vein A and vein B successively appear from top to bottom within the deposit. Andesite is also consistently present across the deposit. This graph is generated using a deterministic interpretive geologic block model.

The third alternative implements a local proportion model (LPM), which involves estimating the proportion of each geological domain based on borehole data at the target simulation blocks (Armstrong et al., 2011). These estimated local proportion models can then be used as soft data in plurigaussian simulation. Fig. 6 demonstrates one realization of each alternative. As seen in Fig. 6a, the alternative one, which uses the global proportion for the truncation rule, fails to adequately model all

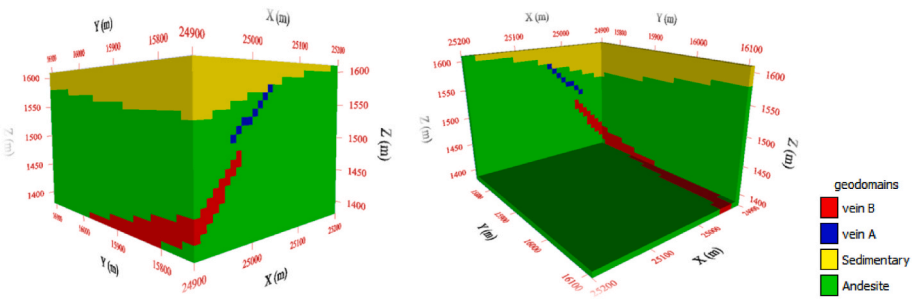

Fig. 3. Block model of the gold deposit: (a) 3D view, (b) cross-sectional view.

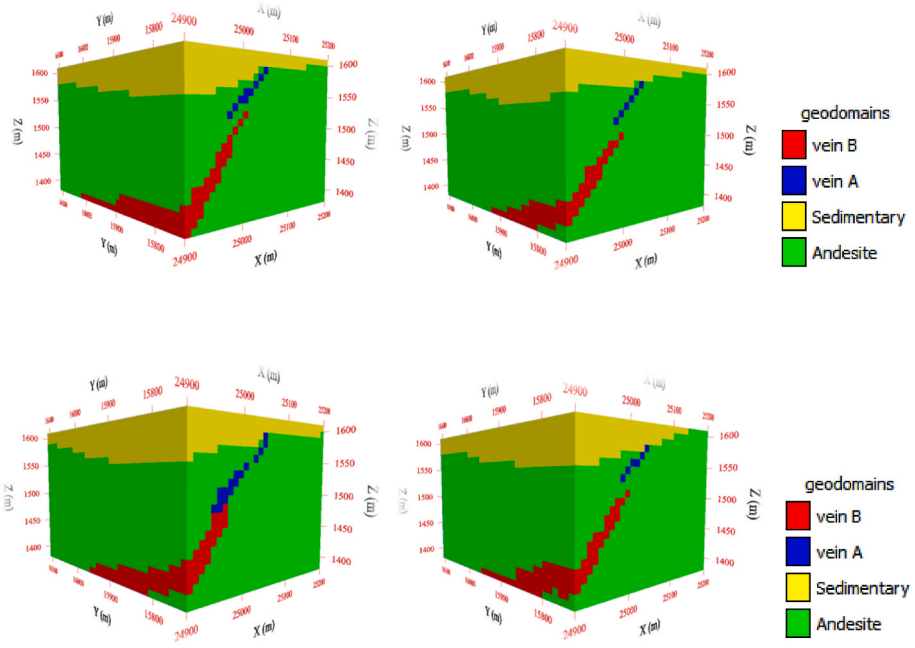

Fig. 4. Four random realizations of vein-type gold deposit obtained from MPS.

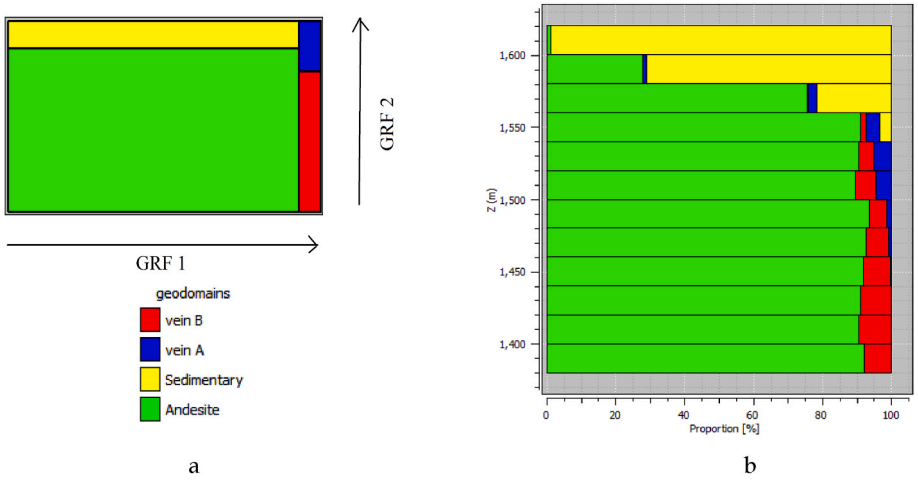

Fig. 5. a) Contact relationship between four geological domains (flag); b) vertical proportion curve of the four geo-domains.

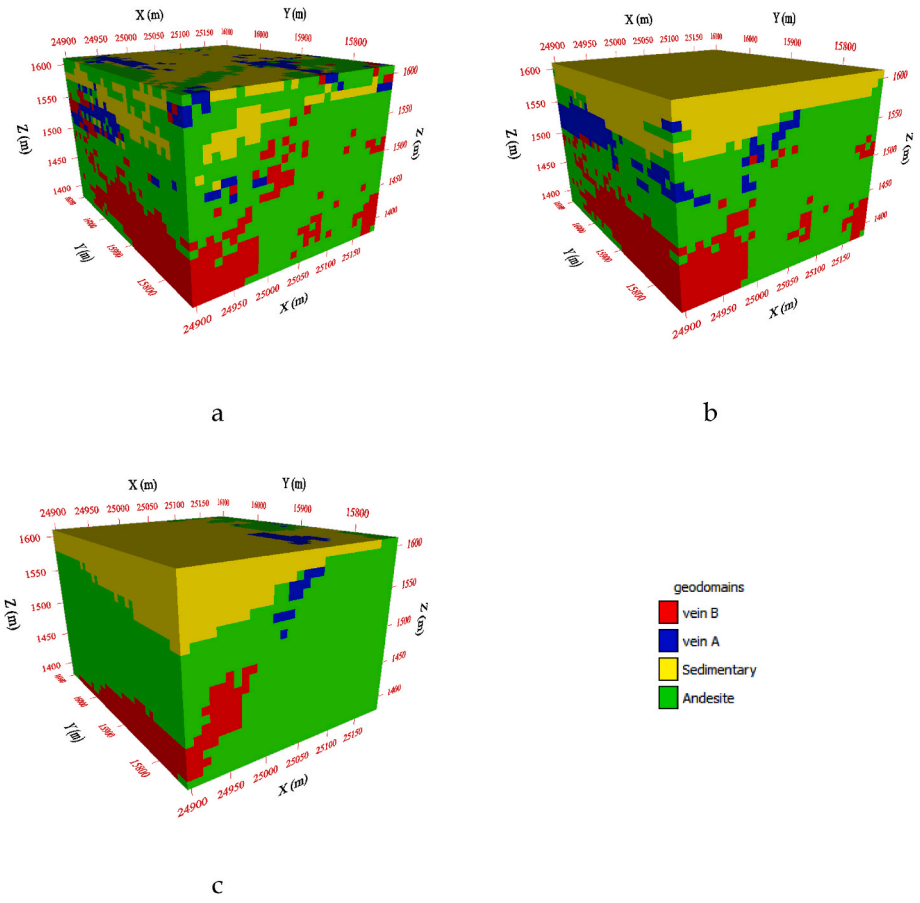

Fig. 6. A realization from a) alternative one: global proportion; b) alternative two: vertical proportion curve; and c) alternative three: local proportion model.

geological domains, resulting in patchy and unstructured geo-domains. Alternative two (Fig. 6b) mimics the vertical fluctuation of the geological domains, consistent with the inferred VPC (Fig. 5b), but it does not accurately capture the narrow structure of the veins. Alternative three (Fig. 5c) shows improved results compared to alternatives one and two. It represents the vertical variation of geological domains. However, it does not properly reproduce the long-range shape of veins, particularly Vein A, which has the smallest proportion.

A useful information that can be derived from the realizations is the transition probabilities, which indicate the frequencies of simulated geodomains between neighboring blocks across the simulation domain and realizations. Tables 1, and 2 represent this information for all three alternatives of the plurigaussian simulations and MPS results, respectively, alongside the interpreted geological block model. Each rock unit is likely to be in contact with every other, except for sedimentary rock and vein B. This distinction is reflected only in alternative two of the plurigaussian simulations results. Alternative one may be affected by insufficient conditioning data, hindering the algorithm from accurately capturing contact relationships. In alternative three, the local proportion calculated from limited conditioning data may explain the minor transition probabilities between these two distinct geodomains. Alternative two accurately reproduces the transition probabilities between andesite and vein B. by incorporating the vertical proportion curve to depict the vertical variation of geodomains due to contact limitation. MPS results show the lowest transition probability between these two geodomains compared to alternatives one and three. Upon comparing the simulation outcomes (Table 1) with the interpretive geological block model (Table 2), it becomes evident that the MPS outcomes better represent the probabilities of transitions between each geodomain.

Table 1
Transition probabilities calculated by considering the simulated geodomains on adjacent blocks (average statistics over 100 realizations).

Plurigaussian simulations (alternative one/two/three)				
When leaving a block of geodomain …	When finds a block belonging to geodomain …			
	Andesite	Sedimentary	Vein A	Vein B
Andesite	0.8727/ 0.9340/ 0.9532	0.0448/ 0.0184/ 0.0122	0.0379/ 0.0108/ 0.0103	0.0446/ 0.0369/ 0.0243
Sedimentary	0.4222/ 0.1555/ 0.1228	0.4998/ 0.8319/ 0.8641	0.0762/ 0.0126/ 0.0116	0.0018/ 0.0000/ 0.0014
Vein A	0.2340/ 0.2332/ 0.2567	0.0506/ 0.0309/ 0.0286	0.5523/ 0.5737/ 0.5699	0.1631/ 0.1622/ 0.1448
Vein B	0.2730/ 0.2283/ 0.2420	0.0011/ 0.0000/ 0.0014	0.1639/ 0.0479/ 0.0584	0.5619/ 0.7238/ 0.6983
MPS				
When leaving a block of geodomain …	When finds a block belonging to geodomain …			
	Andesite	Sedimentary	Vein A	Vein B
Andesite	0.9733	0.0027	0.0065	0.0175
Sedimentary	0.0263	0.9711	0.0022	0.0004
Vein A	0.3539	0.0125	0.5700	0.0636
Vein B	0.2698	0.0007	0.0185	0.7110

3.4. Uncertainty assessment

Once the realizations are ready, one can produce local uncertainty maps. In this regard, by using probability maps, it is feasible to assess the

Table 2
Transition probabilities calculated by considering the interpretive geological block model on adjacent blocks.

Interpretive geological block model				
When leaving a block of geodomain …	When finds a block belonging to geodomain …			
	Andesite	Sedimentary	Vein A	Vein B
Andesite	0.9746	0.0025	0.0071	0.0158
Sedimentary	0.0239	0.9729	0.0032	0.0000
Vein A	0.3254	0.0158	0.5961	0.0627
Vein B	0.2440	0.0000	0.0213	0.7347

degree of uncertainty in rock units at a specific, localized (block-by-block) scale. It is now possible to characterize the geo-domains at each target location in the deposit by their probabilities of occurrence, which are calculated from the frequencies observed over numerous (in this case, 100) conditional realizations.

Before producing such probabilistic maps, the global variation of gold grade is investigated in the four geological domains. Fig. 7 illustrates the boxplots of gold grade in the four geo-domains, where the distributions of gold are shown. It can be seen that the distribution of gold grade in sedimentary rock and andesite is similar in terms of the range of data and median, as well as in veins A and B. Therefore, from the modeling perspective, we are mainly dealing with two main geo-domains: waste and ore. Grouping the geo-domains also makes the analysis of gold more convenient due to the paucity of data in vein A and sedimentary domains. As a result, we will continue the investigation with two major groupings of geological domains. Hence, the probability maps were computed for two main geo-domains (waste and ore) and not for all the geo-domains separately. As mentioned previously, probability maps were calculated by analyzing the frequency of occurrence of each geo-domain across the 100 conditional realizations for each block cell. The more frequently a geo-domain appeared across the ensemble of realizations, the higher the probability that it would be present in a given block. The resulting probability map reflects uncertainty by showing areas with varying levels of risk and expected outcomes.

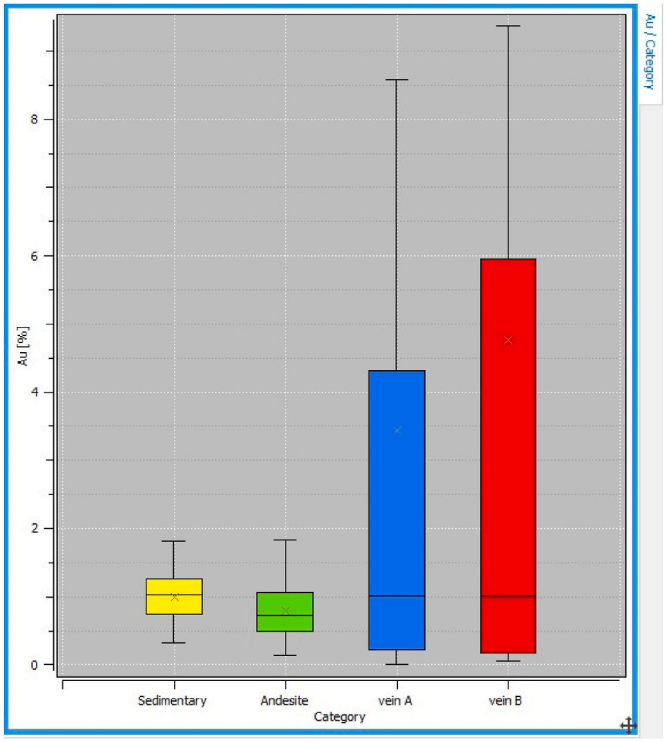

Fig. 7. Boxplots of gold grade for each geo-domain. The whiskers present the minimum of data, 1st, 2nd (median), 3rd quartiles, and maximum of data.

The probability maps provide additional information to the interpreted geological model by highlighting the probability of having the geo-domains of interest (Fig. 8), serving as a supplement to the deterministic model (Fig. 3). This is an improvement over deterministic modeling. Therefore, the probabilities of two geo-domains were obtained from realizations produced by MPS (Fig. 8a) and plurigaussian simulations (Fig. 8b). Alternative three for the latter approach is chosen for further investigation since it looks to generate better outcomes in terms of replicating the long-range structure of geological domains than alternatives one and two. As shown, zones colored in red represent areas with a high probability of containing a specific geo-domain, reflecting a low level of risk of not finding it. Conversely, zones colored in dark blue identify areas with a low probability of finding a specific geo-domain, representing a high level of certainty that the geo-domain will not be present. Zones colored in light blue, green, or yellow represent areas of high boundary uncertainty. The probability maps created from the 100 realizations in Fig. 8a show that the pattern of geological units holds consistent across all simulations, proving that the desired patterns of long connectivity of veins, their forms, and dimensions are reproduced in MPS properly. The probability of ore obtained from plurigaussian simulation illustrates the shape of the veins. However, when compared to the interpretive geological block model, the probability map of ore obtained from MPS is more compatible with our expectations for the shape of veins (ore). MPS takes into account the current geological understanding of the ore body and reflects the uncertainty in the spatial arrangement of the geo-domains boundaries in a better way in terms of reproduction of long-range and shape continuity.

3.5. Statistical validation

After calculating the local uncertainty and presenting it in the format of probability maps, it is important to validate the produced models by comparing them to the interpretive geological block model. For this purpose, the most probable rock unit is calculated and the corresponding most likely category is assigned to each block. For instance, if the probability of ore and waste at the block X is 0.7 and 0.3, respectively, then based on the maximum probability, the ore is assigned to that block. The most likely rock model is then compared block by block with the interpretive geological block model. Specifically, when a block in the stochastic model shows the same rock unit as in the interpretive geological block model, a “match” category is assigned; otherwise, a “mismatch” category is assigned. As can be observed, the MPS results (Fig. 9a) more closely resemble the interpretive geological block model than the plurigaussian simulations (the alternative three) (Fig. 9b), primarily due to the higher percentage of matching blocks across the vein’s boundaries.

To evaluate the generated models, the MPS and plurigaussian simulations are compared in terms of their ability to replicate the declustered proportions of ore (Vein A and Vein B) and waste (Sedimentary and Andesite) (Fig. 10). The results indicate that MPS outperforms plurigaussian simulations in accurately reproducing these proportions. Plurigaussian simulations face challenges in this deposit, particularly in accurately replicating the original declustered proportions of ore and waste, due to several factors. Firstly, the heterogeneous nature of veins, often characterized by complex geological structures within the ore zone, poses a significant obstacle. Secondly, the limited availability of drill-hole data may not adequately capture the anticipated long-range structure of the veins. In contrast, MPS employs a sophisticated modeling approach that considers higher-order patterns and structures of geological data to effectively reproduce the original declustered proportions. Additionally, MPS uses a TI as a reference for simulating patterns and features observed in the original data, which proves highly effective, especially in cases of data scarcity.

Exploring the spatial contiguity of the ore domain within this deposit can provide valuable insights. It is crucial that the chosen geostatistical

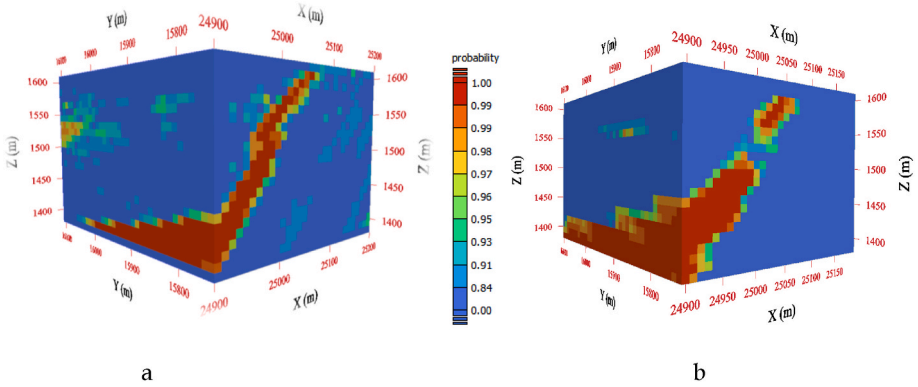

Fig. 8. Probability model of ore, obtained from a set of 100 conditional simulations of a) MPS; and b) plurigaussian simulations.

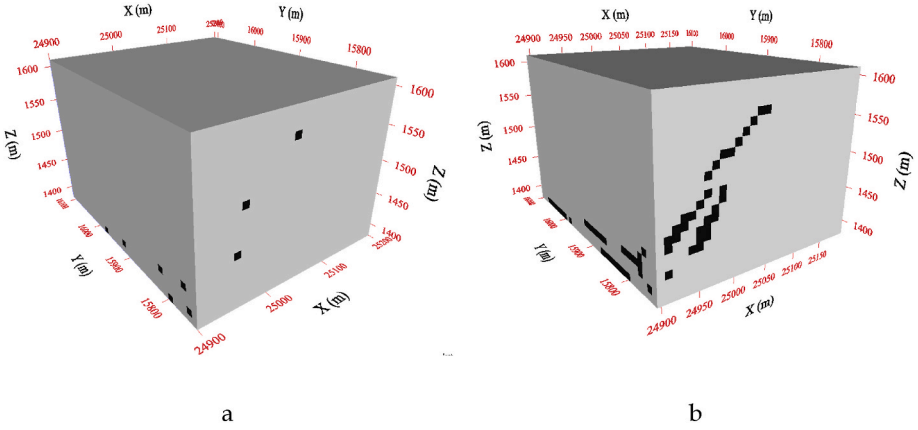

Fig. 9. Match (gray blocks) and mismatch (black block) visualization for the results obtained from a) MPS, b) plurigaussian simulations.

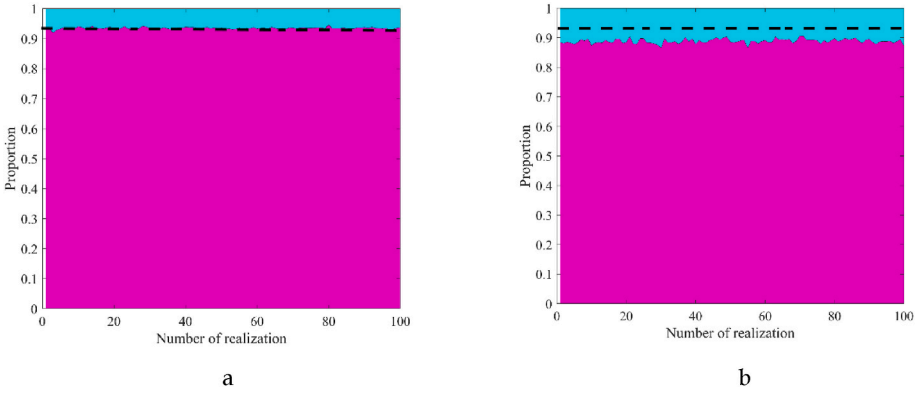

Fig. 10. Proportion reproduction of ore and waste throughout the realizations obtained from a) MPS; and b) plurigaussian simulations; the dashed line represents the original declustered proportions of waste.

modeling approach accurately represents the ore domain (veins) with enhanced interconnectivity or spatial contiguity. This approach would yield a more condensed and contiguous simulated ore domain at the target grid nodes. To achieve this, we employed the connectivity function (Renard and Allard, 2013) as a multiple-point statistic to quantify the likelihood that a grid node is connected with another grid node situated at a lag separation distance (h) within the same ore domain. Consequently, the probability of connectivity between any two grid nodes can be expressed as a function of h, illustrated here for the ore domain across Easting (X), Northing (Y), and Vertical (Z) directions (Fig. 11). Connectivity functions were computed across individual realizations of plurigaussian simulations and MPS, averaged, and then compared with the function derived from the interpretive geological block model. As shown in this figure, MPS demonstrates greater compatibility with the interpretive geological block model in terms of connectivity metrics compared to plurigaussian simulation results.

Another approach to evaluate the efficacy of the proposed method is to analyze the reproducibility of initial variograms for ore and waste zones. Indicator variograms were computed for indicators associated with the ore domain in the Easting (X), Northing (Y), and Vertical (Z) directions. The experimental variograms of the indicators from the interpretive geological block model were compared with those derived from the corresponding average variogram generated by plurigaussian simulations and MPS (Fig. 12). As observed, MPS results exhibit superior

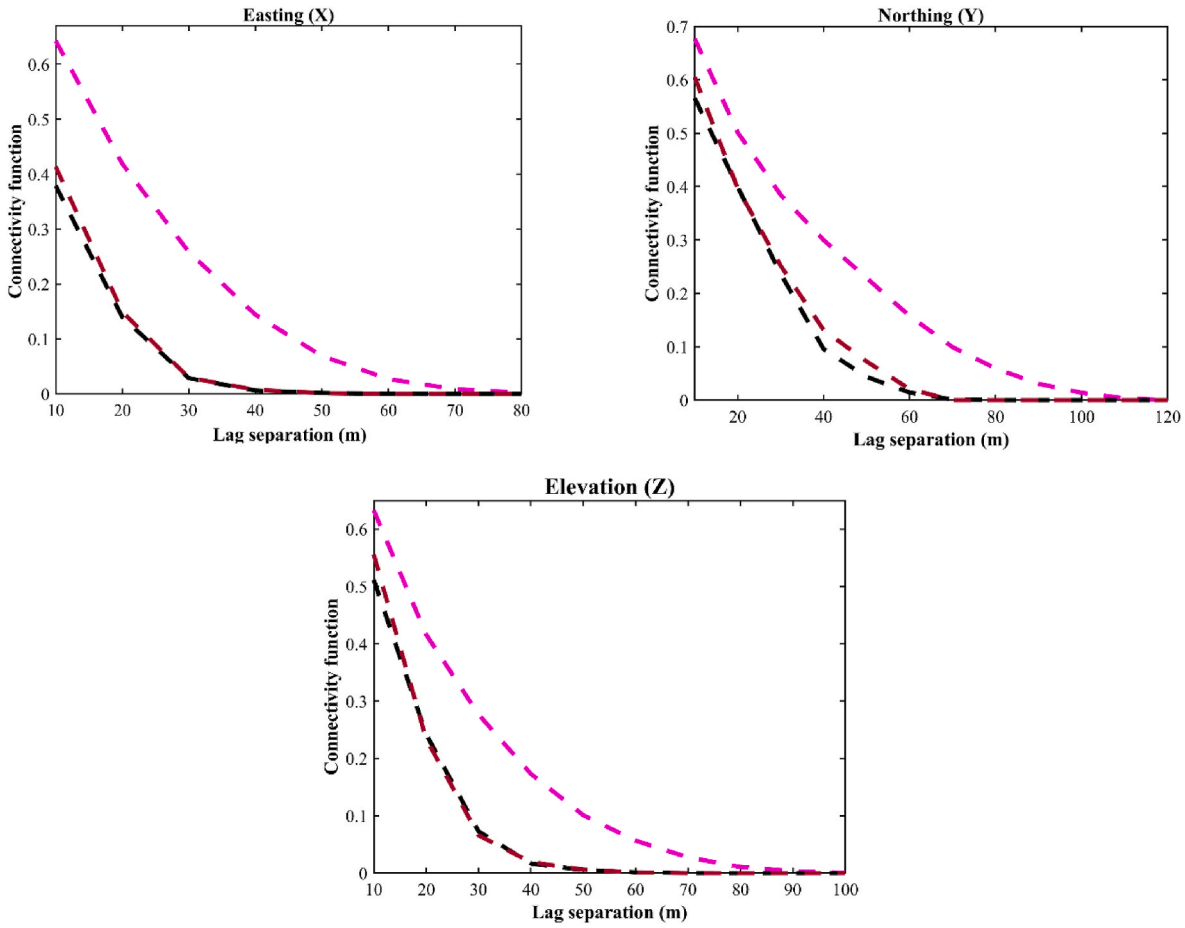

Fig. 11. Connectivity measures as a function of lag separation along Easting (X), Northing (Y), and Elevation (Z) for the ore domain. Dashed magenta line: average of connectivity measures obtained from plurigaussian simulation results, dashed dark red line: average of connectivity measures obtained from MPS results, and dashed black line: connectivity measures obtained from interpretive geological block model.

reproduction of the indicator variograms. Plurigaussian simulation results demonstrate a notable bias despite the incorporation of spatial continuity into the modeling procedure.

3.6. Grade modeling

The cascade modeling approach used in this study relies on predictive models of grades and also a probabilistic description of each geodomain. These uncertainty models are produced using MPS and plurigaussian simulations, providing the probability of ore and waste are available at each target block. Before obtaining the final grade estimate model, it is essential to generate predictive models of ore and waste in each block. To achieve this, the gold grade values from datasets belonging to ore and waste were initially separated. For generation of the grade estimate model, which is a mathematical or computational tool used to predict the spatial distribution of grades, various deterministic interpolation techniques can be employed. The initial experimental variogram analysis did not reveal a distinct structure in the raw gold grade ore data. However, upon transformation to normal scores, a satisfactory structure emerged. This transformation indicated satisfactory variograms at this Gaussian scale.

After transforming the data to normal scores, separate variogram models were computed for the two geodomains: one for the ore dataset and another for the waste dataset, given the expected differences in the spatial variability of the grade between these two domains.

The variogram models were calculated using a lag distance of 15 m and a tolerance of 7.5 m. Due to limited data availability in different directions (Appendix 1, Fig. 16), omnidirectional experimental variograms were computed for both ore and waste, and variogram models were fitted accordingly (Fig. 13):

$$\gamma_{ore} = 0.83nugget + 0.15Sph(14.94m)$$

$$\gamma_{waste} = 0.5nugget + 0.53Cubic(132.907m)$$

In the next step, using the conditional data and the variogram models, 100 realizations of the gold variable (for each ore and waste domain) were generated by using the SGS approach. The most likely E-type maps were created by averaging the 100 simulation results and contrasting them with the most likely gold veins model obtained in the preceding steps. As a result, two SGS E-type values are now available at each block location, whether it is ore or waste after back-transforming to the original scales. Therefore, predictive grades required in Eq. (1) were available with $k = 2$ throughout the deposit. Then, each predictive model was multiplied by the probability of occurrence of the specific geological domain (ore or waste) and the final results were obtained after summing up the four values as in Eq. (1).

To evaluate the outcomes, three distinct cases are contrasted in the following sections:

Case I. Predictive gold models were developed using SGS and the probability of ore and waste geological domains acquired from MPS.

Case II. Predictive gold models were developed using SGS and the probability of ore and waste geological domains acquired from plurigaussian simulations (only alternative three).

Case III. Predictive gold models were developed using SGS in each

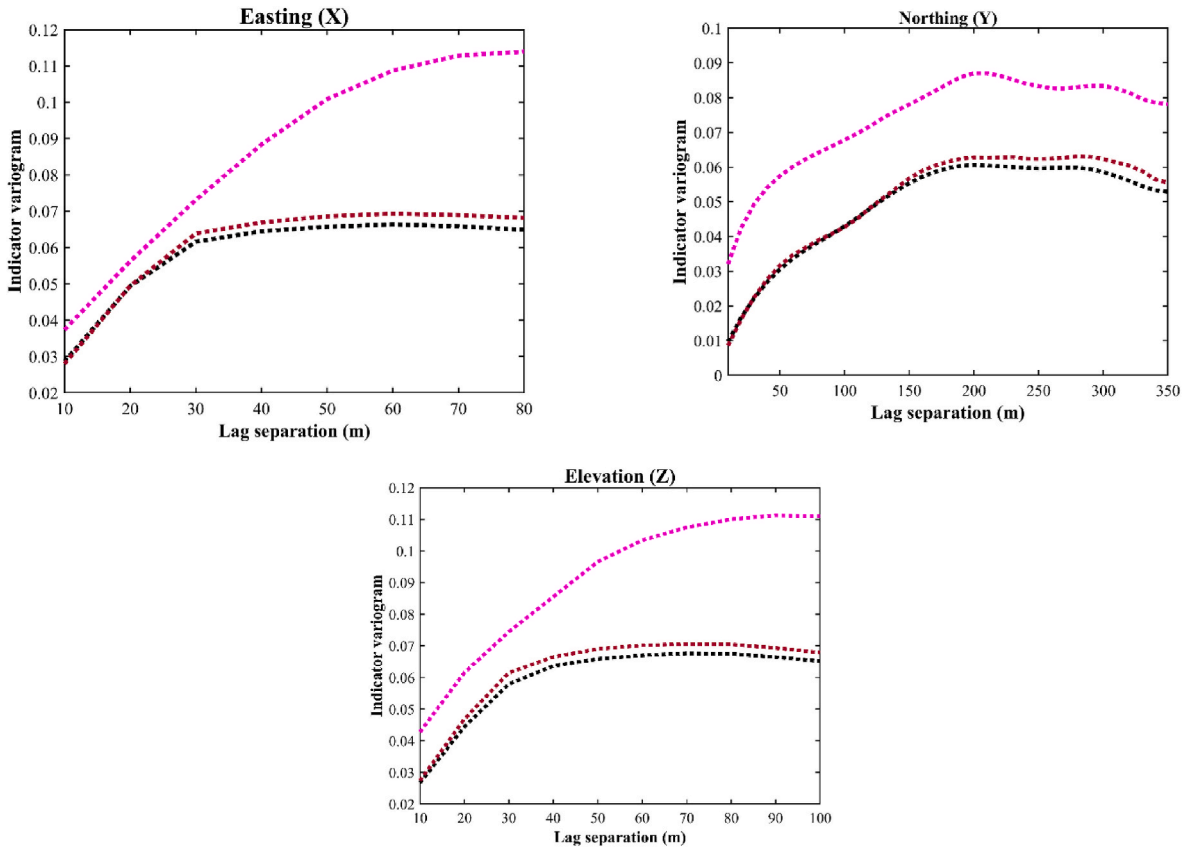

Fig. 12. Indicator variograms as a function of lag separation along Easting (X), Northing (Y), and Elevation (Z). Dashed magenta line: average of indicator variograms obtained with 100 realizations of plurigaussian simulations, Dashed dark red line: average of indicator variograms obtained with 100 realizations of MPS, and Dashed black line: indicator variograms calculated over the interpretive geological block model.

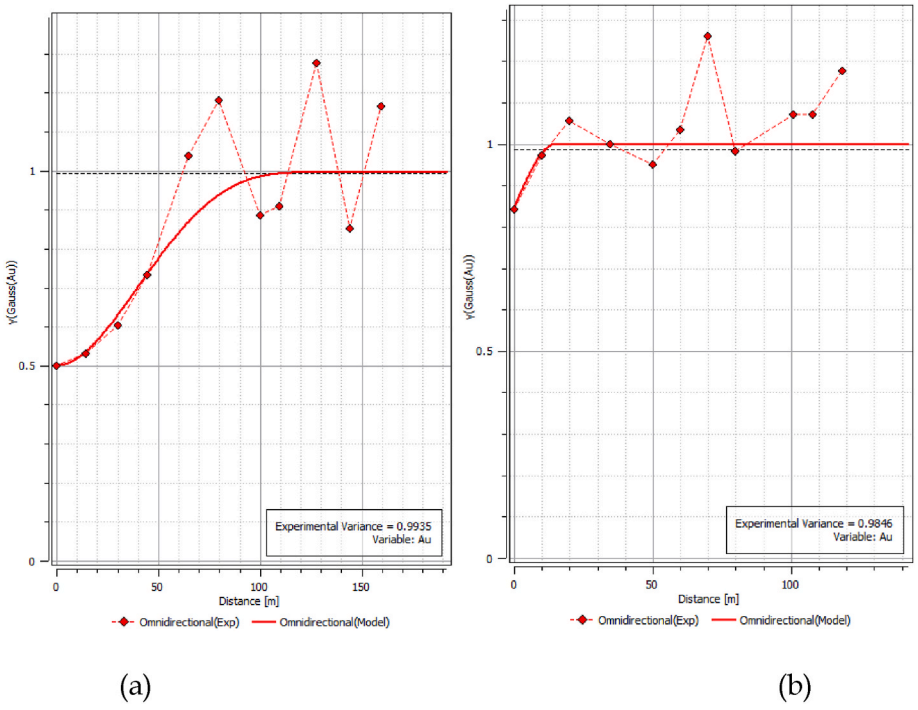

Fig. 13. Omnidirectional variograms for gold grade in (a) waste, (b) ore.

domain of the interpretive geological domain separately, implying traditional cascade modeling.

Case IV. Predictive gold models were developed using SGS without separating the data into ore and waste, and the geological information was neglected.

The third case represents the traditional cascade modeling of ore grades, where the deposit is first split into ore and waste, and the gold grade is estimated or simulated inside each domain independently. The fourth case serves to highlight the significance of confining simulations within homogeneous domains, emphasizing the ineffectiveness of disregarding geological factors.

3.7. Application to mineral resource evaluation

Fig. 14 represents the obtained results of produced models using probabilistic modeling and deterministic approaches. As can be seen, the model obtained via case I accurately and realistically reproduced the gold grade along the vein continuity (Fig. 14a). Although case II mimicked the shape of the veins to some extent, it suffers from insufficient continuity in grade estimation, where the gold grade in the vein appears slightly disseminated (Fig. 14b).

Case III (Fig. 14c) represents the traditional cascade modeling for such a deposit with vein structures. While the gold grade follows the shape of the veins, it shows the hard boundary of gold grade variation around the veins. As illustrated, the deterministic approach in case IV (Fig. 14d) is also unable to properly replicate the vein structures along the geo-domain layout, causing significant inaccuracies in the morphology of the orebody.

Table 3 shows the statistical parameters obtained from Cases I, II, III, and IV for the final predictive model of gold grade in ore zones. As can be seen, Case IV, where the impact of geological domains is ignored, shows a significant underestimation of high values. However, the other cases properly reproduce the high values. In addition, Cases III and IV illustrate the lowest variances, implying a higher smoothing effect compared to Cases I and II, which exhibit less smoothing effect.

Fig. 15 illustrates the recoverable functions derived from Cases I, II, III, and IV, representing the final predictive gold grade within the ore zone block model. As evident from the figures, Cases I and II exhibit strikingly similar results in tonnage (Fig. 15a) and metal quantity (Fig. 15c), whereas Cases III and IV demonstrate the highest and lowest values for both tonnage and metal quantity. There are notable distinctions in the mean grade above cutoffs among the cases, with Case IV notably exhibiting a pronounced smoothing effect.

Table 3
Statistical parameters of final predictive model of gold grade in ore zone, and original boreholes.

Gold grade (ore)- ppm	Mean	Variance	Minimum	Maximum
Drillhole sample points	4.07	43.61	0.00	30.30
Case I	3.17	1.90	0.05	29.41
Case II	3.10	1.73	0.00	30.30
Case III	4.13	1.44	0.00	30.30
Case IV	1.75	0.26	0.29	5.78

4. Discussion

This study demonstrates a potential workflow for modeling a vein-type gold deposit. It begins by employing MPS to construct the geological domains, followed by establishing the predictive model for estimating the final gold grade, incorporating the probabilistic definition of these geological domains. This work provides insights into the implementation details of the proposed algorithm for these type of deposits, which exhibits long-range geological structures such as veins. For this purpose, a reliable implicit geological modeling approach is required to establish an interpretive geological model that aligns with the geological settings of the deposit being studied.

Implicit geological modeling provides several benefits, including the ability to quickly generate models by deducing geological contacts from limited data, integrating numerous data types for thorough interpretations, analyzing uncertainties, and reducing the need for manual involvement through automation. Explicit geological modeling can also be utilized, but it may have challenges in effectively representing intricate geological characteristics, especially when the input data is

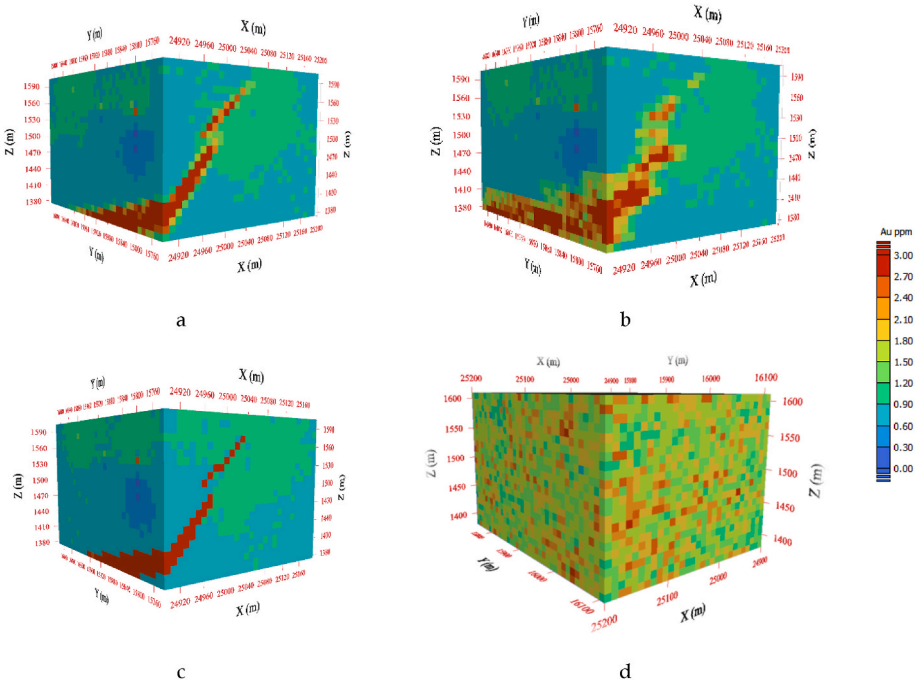

Fig. 14. Final grade model using cascade approach with probability driven from a) Case I (MPS), b) Case II (plurigaussian simulations), c) Case III (traditional cascade modeling)), and d) Case IV (without considering any geological controls).

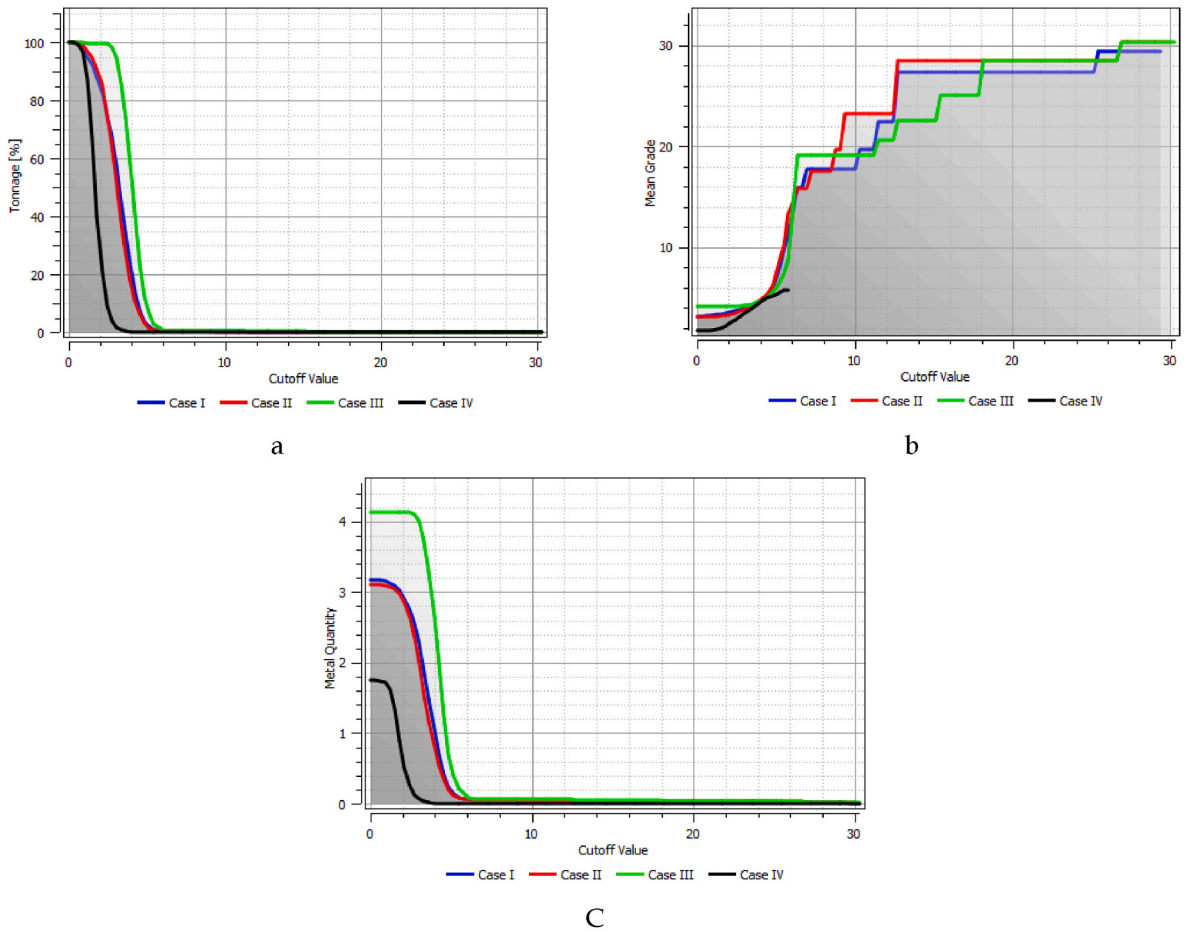

Fig. 15. Recoverable functions over the final predictive model of gold grade in ore zone for a) tonnage-cutoff, b) mean grade-cutoff, c) metal quantity-cutoff.

limited (such as in this study), which could result in less accurate geological interpretations. In addition, explicit modeling may necessitate a significant level of skill to accurately parameterize and comprehend outcomes, hence restricting its accessibility to individuals lacking specialized experience.

The produced implicit geological model can then be used as a TI to generate the stochastic geological model of the deposit using the DeeSse algorithm, which is an MPS-based algorithm.

We utilized the constructed TI as the interpretive geological block model. This method requires drill-hole data and basic geological comprehension. Although there are numerous advantages to generating TI using borehole data, there may be some legitimate criticisms of this method. Borehole data usually encompasses a restricted area and might not fully represent the geological heterogeneity in the subsurface. Biases in data collection or interpretation might cause inaccuracies or artifacts in the training image, impacting the reliability of simulations. Limited borehole data can complicate the representation of geological features and interactions, leading to overly simplistic or inaccurate training representations. The discrete nature of borehole data, offering point measurements rather than continuous spatial information, may pose challenges in faithfully capturing the continuity and spatial correlation of geological features within a training image, especially in regions with sparse data coverage. Overall, using borehole data to create a training image has advantages in terms of geological realism and direct representation of field observations. However, it is crucial to consider the limitations and potential biases of the data source to maintain accuracy and reliability in modeling. By combining borehole data with other geological information sources and implementing suitable quality control procedures, it is possible to lessen these restrictions and improve the effectiveness of training images in geological modeling applications.

The DeeSSe method offers numerous benefits in geological modeling. This approach provides realistic depictions of geological formations by integrating various forms of input data tools for probabilistic modeling. DeeSSe effectively manages intricate geological scenarios, facilitating the observation and interpretation of geological models. Its interpretive flexibility allows users to incorporate their geological knowledge, thereby aiding decision-making in mineral exploration and mine planning. DeeSSe enhances comprehension and evaluation of geological characteristics, promoting well-informed decision-making in the resource sector. Despite these advantages, the DeeSSe algorithm also has limitations. Firstly, it requires significant processing resources due to its complex nature, which may limit access for users with limited computing capabilities in large-scale deposits. Furthermore, the process of parameter adjustment can be labor-intensive and requires expertise in both geology and computational modeling. Model validation can be challenging, especially when ground truth data are scarce. Additionally, the accuracy of its output depends on the quantity of the input data, potentially leading to discrepancies in the generated geological models.

Despite these challenges, a thorough examination of these parameters can help alleviate the constraints of the DeeSSe algorithm in geological modeling applications.

Due to the lack of stationarity in that specific case study, it is not feasible to conduct a reliable cross-validation exercise. Stationarity, which assumes that the statistical properties of the system do not change over space, is a fundamental requirement for many modeling techniques. In its absence, the model's predictions may not be consistent or accurate across different regions of the study area. Consequently, it becomes challenging to demonstrate the correctness of the uncertainty

assessment using proper scoring rules, which are statistical tools used to evaluate the accuracy of probabilistic predictions. Without stationarity, the variability in the data can lead to misleading results, undermining the validity of the scoring rules.

Additionally, the same problem arises with the plurigaussian technique. This method also relies on the assumption of stationarity to effectively model the spatial distribution of geological features. In this specific case study, the lack of stationarity compromises the ability of the plurigaussian technique to accurately represent the uncertainty, further complicating the validation of the uncertainty assessment. As a result, both MPS and plurigaussian methods face significant challenges in this context, highlighting the need for alternative approaches or additional data to address the issue of non-stationarity and cross-validation.

In this study, SGS was utilized to support the predictive model outlined in Eq. (1). This decision was based on the observation that the distribution of gold grade within the ore zone lacked a discernible structure on its original scale, making the application of simple or ordinary kriging impractical. However, by transforming the data into normal scores, it became feasible to fit a variogram model to the experimental variograms. This adjustment was necessary due to the limited availability of data, with only 82 samples of gold grade in the ore zone. Therefore, Gaussian-based geostatistical methods are preferred under such circumstances. Additionally, alternative approaches such as multi-Gaussian kriging may also be considered viable alternatives.

5. Conclusion

This study aimed to model a vein-type gold deposit with long-range features using multiple-point geostatistical simulation. Modeling the structure of veins poses a challenge due to their complex geometry, which often widens in two dimensions while remaining narrow in the third dimension, making it difficult for mine geologists to explicitly evaluate their layout. Geological modeling typically involves deterministic interpretation and definition of primary lithological zones, utilizing insights from geological experts and drill-hole samples. This technique requires a thorough understanding of the geology of the ore deposit before grade estimation and further mine planning. However, there is always uncertainty regarding the actual extent of the lithological zones. Failure to consider geological control can reduce the accuracy of the final grade model. A probabilistic technique has been proposed as a solution to this issue, involving geostatistical simulation of geo-domains, using the MPS approach, and comparing the results to those of plurigaussian simulations. The reason for using Multiple-Point Statistics (MPS) was not merely to ensure the conditioning of the model, but rather to provide a comprehensive representation of uncertainty. By leveraging MPS, the approach captures the complex spatial relationships and variability inherent in geological formations, offering a more detailed and accurate model of uncertainty compared to traditional methods. This allows for a better understanding of the potential range of geological scenarios, ultimately leading to more informed decision-making in geological modeling and resource estimation.

Through various evaluation methodologies, the results demonstrated that MPS outperformed the plurigaussian simulations. In MPS, the shape of veins was replicated more accurately, aligning better with the interpretive geological block model produced by implicit modeling. This was confirmed using match/mismatch maps and geological proportion reproduction. Once the probabilistic description of geological domains was established, the predictive gold grade estimates were compared across three cases. It was shown that the gold grade is better modeled along the veins when we used the MPS results. For future work, the method can be extended to apply other MPS algorithms such as SNESIM and Filtersim for geological domaining and other methods for modeling the gold grade such as turning bands simulation (Emery, 2008).

CRediT authorship contribution statement

Aida Zhexenbayeva: Writing – original draft, Visualization, Validation, Software, Formal analysis. **Nasser Madani:** Writing – review & editing, Writing – original draft, Validation, Supervision, Project administration, Methodology, Investigation, Funding acquisition, Data curation, Conceptualization. **Philippe Renard:** Writing – review & editing, Software, Methodology, Investigation, Funding acquisition. **Julien Straubhaar:** Writing – review & editing, Software, Methodology.

Declaration of competing interest

The authors declare the following financial interests/personal relationships which may be considered as potential competing interests: Nasser Madani reports financial support was provided by Swiss State Secretariat for Education Research and Innovation.

Data availability

The authors do not have permission to share data.

Acknowledgement

The first and second authors are grateful to Nazarbayev University for funding this work via Faculty Development Competitive Research Grants for 2021–2023 under Contract No. 021220FD4951. The second, third, and fourth authors also acknowledge the Swiss State Secretariat for Education, Research, and Innovation for partially funding this work under contract No. SFG 607. The authors also acknowledge the editorial board and two anonymous reviewers for their invaluable efforts toward improving the overall scientific quality of this manuscript.

Appendix 1

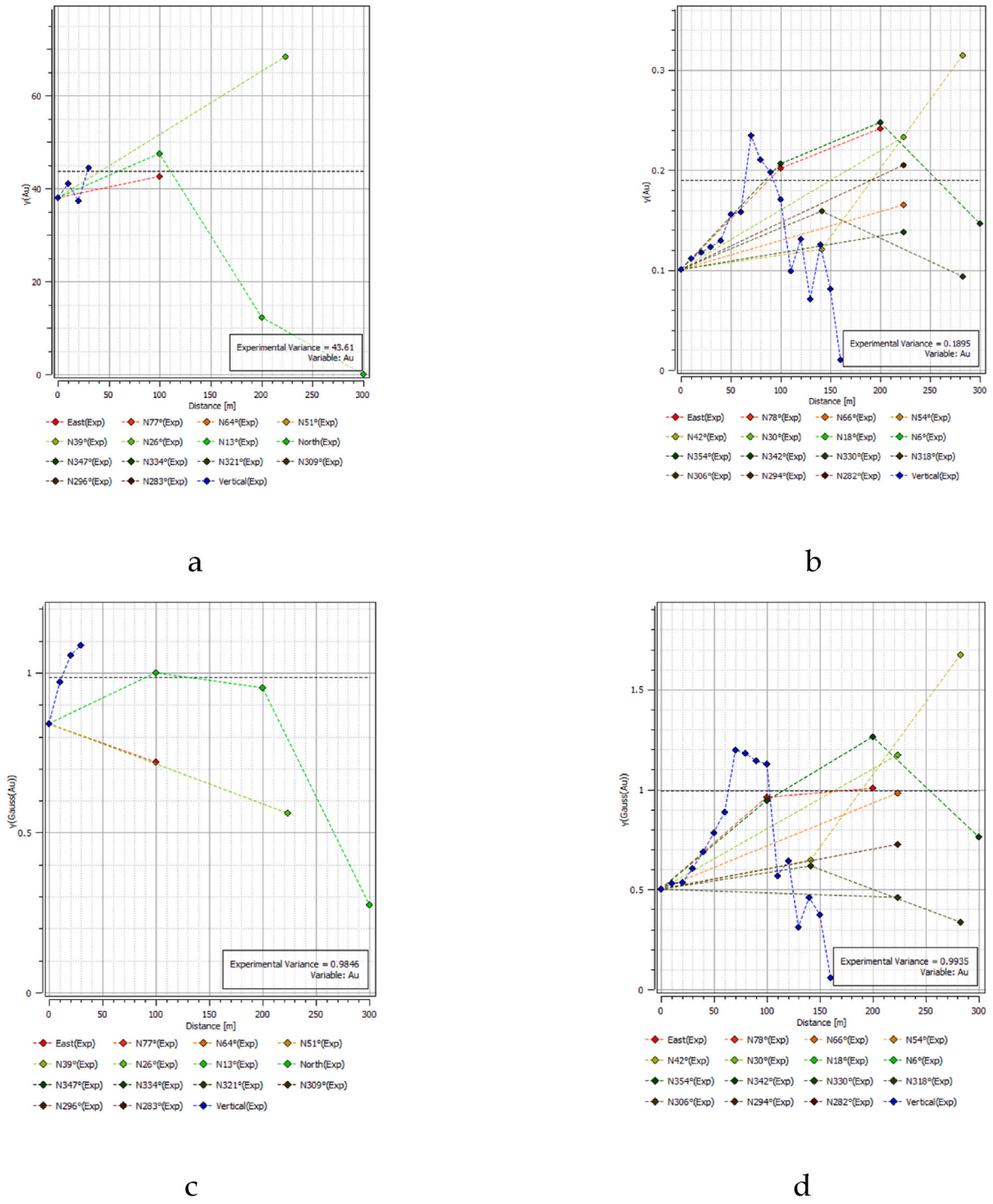

Fig. 16. Experimental variograms in different directions for gold grade-ore (a: original scale; b: nscores) and for gold grade-waste (c: original scale; d: nscores).

References

Abulkhair, S., Madani, N., 2022. Stochastic modeling of iron in coal seams using two-point and multiple-point geostatistics: a case study. Mining, Metallurgy & Exploration 39 (3), 1313–1331.

Alabert, F.G., Massonnat, G.J., 1990. Heterogeneity in a complex turbiditic reservoir: stochastic modelling of facies and petrophysical variability. In: 65th Annual Technical Conference and Exhibition. Society of Petroleum Engineers, pp. 775–790, 1990, SPE Paper Number 20604.

Anderson, K.S., Hickson, T.A., Crider, J.G., Graham, S.A., 1999. Integrating teaching with field research in the Wagon rock project. J. Geosci. Educ. 47, 227–235. https://doi.org/10.5408/1089-9995-47.3.227.

Armstrong, M., Galli, A., Beucher, H., Le Loc'h, G., Renard, D., Renard, B., Eschard, R., Geffroy, F., 2011. Plurigaussian Simulations in Geosciences. Springer, Berlin.

Arpat, G.B., Caers, J., 2007. Conditional simulation with patterns. Math. Geol. 39, 177–203. https://doi.org/10.1007/s11004-006-9075-3.

Avalos, S., Ortiz, J.M., 2020. Recursive convolutional neural networks in a multiple-point statistics framework. Comput. Geosci. 141, 104552 https://doi.org/10.1016/j.cageo.2020.104522.

Bai, T., Tahmasebi, P., 2020. Hybrid geological modeling: combining machine learning and multiple-point statistics. Comput. Geosci. 142, 104519 https://doi.org/10.1016/j.cageo.2020.104519.
Bastante, F.G., Ordóñez, C., Taboada, J., Matías, J.M., 2008. Comparison of indicator kriging, conditional indicator simulation and multiple-point statistics used to model slate deposits. Eng. Geol. 98 (1–2), 50–59. https://doi.org/10.1016/j.enggeo.2008.
Bayer, P., Huggenberger, P., Renard, P., Comunian, A., 2011. Three-dimensional high resolution fluvio-glacial aquifer analog: Part 1: field study. J. Hydrol. 405 (1–2), 1–9. https://doi.org/10.1016/j.jhydrol.2011.03.038.
Boisvert, J., 2010. Geostatistics with Locally Varying Anisotropy. University of Alberta, p. 175p. Ph.D. Dissertation.
Boisvert, J.B., Pyrcz, M.J., Deutsch, C.V., 2007. Multiple-point statistics for training image selection. Nat. Resour. Res. 16, 313–321.
Boucher, A., Costa, J.F., Rasera, L.G., Motta, E., 2014. Simulation of geological contacts from interpreted geological model using multiple-point statistics. Math. Geosci. 46, 561–572.
Boucher, A., Dimitrakopoulos, R., 2012. Multivariate block-support simulation of the Yandi iron ore deposit, Western Australia. Math. Geosci. 44 (4), 449–468.
De Iaco, S., Maggio, S., 2011. Validation techniques for geological patterns simulations based on variogram and multiple-point statistics. Math. Geosci. 43, 483–500. https://doi.org/10.1007/s11004-011-9326-9.
Deutsch, C.V., Journel, A.G., 1998. GSLIB: geostatistical library and user's guide. In: Applied Geostatistics, Journel, AG. Oxford University.
Deutsch, C.V., 1992. Annealing Techniques Applied to Reservoir Modeling and the Integration of Geological and Engineering (Well Test) Data. Stanford University. Doctoral dissertation.
Deutsch, C.V., Wang, L., 1996. Hierarchical object-based stochastic modeling of fluvial reservoirs. Math. Geol. 28, 857–880. https://doi.org/10.1007/BF02066005.
Dubrule, O., 2017. Indicator variogram models: do we have much choice? Math. Geosci. 49 (4), 441–465.
Emery, X., Lantuejoul, C., 2014. Can a training image be a substitute for a random field model? Math. Geosci. 46, 133–147.
Emery, X., 2008. A turning bands program for conditional co-simulation of cross-correlated Gaussian random fields. Comput. Geosci. 34 (12), 1850–1862. https://doi.org/10.1016/j.cageo.2007.10.007.
Emery, X., Gonz'alez, K.E., 2007. Probabilistic modelling of lithological domains and its application to resource evaluation. J. S. Afr. Inst. Min. Metall 107 (12), 803–809.
Franke, R., 1982. Smooth interpolation of scattered data by local thin plate splines. Comput. Math. Appl. 8 (4), 273–281.
Geovariances, 2024. Help center. Retrieved from. https://www.geovariances.com/en/?s=help.
Goodfellow, R., Consuegra, F.A., Dimitrakopoulos, R., Lloyd, T., 2012a. Quantifying multi-element and volumetric uncertainty, Coleman McCreedy deposit, Ontario, Canada. Comput. Geosci. 42, 71–78.
Goodfellow, R., Consuegra, F.A., Dimitrakopoulos, R., Lloyd, T., 2012b. Quantifying multi-element and volumetric uncertainty, Coleman McCreedy deposit, Ontario, Canada. Comput. Geosci. 42, 71–78. https://doi.org/10.1016/j.cageo.2012.02.018.
Goovaerts, P., 1997. Geostatistics for Natural Resource Evaluation. Oxford University Press, New York.
Guardiano, F., Srivastava, M., 1993a. Multivariate geostatistics: beyond bivariate moments. In: Soares, A. (Ed.), Geostatistics-Troia. Kluwer Academic, Dordrecht.
Guardiano, F.B., Srivastava, R.M., 1993b. Multivariate geostatistics: beyond bivariate moments. In: Geostatistics Troia'92. Springer, pp. 133–144.
Hardy, R.L., 1971. Multiquadric equations of topography and other irregular surfaces. J. Geophys. Res. 76 (8), 1905–1915.
Houlding, S.W., 1994. 3D Geoscience Modeling, Computer Techniques for Geological Characterization. Springer, New York, p. 321.
Jones, P., Douglas, I., Jewbali, A., 2013. Modeling combined geological and grade uncertainty: application of multiple-point simulation at the Apensu gold deposit, Ghana. Math. Geosci. 45 (8), 949–965.
Journel, A.G., Huijbregts, Ch J., 1978. Mining Geostatistics. Academic Press, London, p. 600.
Journel, A.G., Gómez-Hernández, J.J., 1993. Stochastic imaging of the Wilmington clastic sequence. SPE Form. Eval. 8 (1), 33–40.
Madani, N., 2021. Plurigaussian simulations. In: Daya Sagar, B., Cheng, Q., McKinley, J., Agterberg, F. (Eds.), Encyclopedia of Mathematical Geosciences; Encyclopedia of Earth Sciences Series. Springer, Cham, Switzerland.
Madani, N., Emery, X., 2015. Simulation of geo-domains accounting for chronology and contact relationships: application to the Río Blanco copper deposit. Stoch. Environ. Res. Risk Assess. 29 (8), 2173–2191.
Madani, N., Maleki, M., Emery, X., 2019. Nonparametric geostatistical simulation of subsurface facies: tools for validating the reproduction of, and uncertainty in, facies geometry. Nat. Resour. Res. 28, 1163–1182. https://doi.org/10.1007/s11053-018-9444-x.
Mallet, J.L., 1992. Discrete smooth interpolation. Comput. Aided Des. 24 (4), 263–270.
Mallet, J.L., 2002. Geomodeling. Oxford University Press, New York, p. 624.
Mariethoz, G., 2018. When should we use multiple-point geostatistics? In: Daya Sagar, B., Cheng, Q., Agterberg, F. (Eds.), Handbook of Mathematical Geosciences. Springer, Cham, pp. 645–653.
Mariethoz, G., Caers, J., 2014. Multiple-point Geostatistics: Stochastic Modeling with Training Images. John Wiley & Sons.
Mariethoz, G., Renard, P., Straubhaar, J., 2010. The Direct Sampling method to perform multiple-point geostatistical simulations. Water Resour. Res. 46 (11).
Paithankar, A., Chatterjee, S., 2018. Grade and tonnage uncertainty analysis of an African copper deposit using multiple-point geostatistics and sequential Gaussian simulation. Nat. Resour. Res. 27, 419–436. https://doi.org/10.1007/s11053-017-9364-1.
Pyrcz, M.J., Boisvert, J.B., Deutsch, C.V., 2008. A library of training images for fluvial and deepwater reservoirs and associated code. Comput. Geosci. 34 (5), 542–560. https://doi.org/10.1016/j.cageo.2007.05.015.
Pyrcz, M.J., Boisvert, J.B., Deutsch, C.V., 2009. ALLUVSIM: a program for event-based stochastic modeling of fluvial depositional systems. Comput. Geosci. 35 (8), 1671–1685. https://doi.org/10.1016/j.cageo.2008.09.012.
Quigley, M., Dimitrakopoulos, R., Grammatikopoulos, T., 2018. Risk-resilient mine production schedules with favourable product quality for rare earth element projects. Min. Technol. 127 (1), 41–55.
Rezaee, H., Asghari, O., Koneshloo, M., Ortiz, J.M., 2014. Multiple-point geostatistical simulation of dykes: application at Sungun porphyry copper system, Iran. Stoch. Environ. Res. Risk Assess. 28, 1913–1927.
Renard, P., Allard, D., 2013. Connectivity metrics for subsurface flow and transport. Adv. Water Resour. 51, 168–196.
Robles-Stefoni, L., Dimitrakopoulos, R., 2016. Stochastic simulation of the Fox kimberlitic diamond pipe, Ekati mine, Northwest Territories, Canada. J. S. Afr. Inst. Min. Metall 116 (2), 189–200.
Roldão, D., Ribeiro, D., Cunha, E., Noronha, R., Madsen, A., Masetti, L., 2012. Combined use of lithological and grade simulations for risk analysis in iron ore, Brazil. In: Abrahamsen, P., Hauge, R., Kolbjørnsen, O. (Eds.), Geostatistics Oslo 2012. Springer, Berlin, pp. 423–434.
Rossi, M.E., Deutsch, C.V., 2014. Mineral Resource Estimation. Springer, New York, NY, USA, p. 332.
Seequent, 2022. Leapfrog geo, Version 2021.2.4. https://www.seequent.com/category/products-and-solutions/leapfrog-geo/.
Silva, D.A., Palmer, K.J., Deutsch, C.V., 2015. Spatial modelling of geological domains with multiple training images: application to the Red Dog mine, Alaska, United States. CIM Journal 6 (3), 137–148.
Silva, D.A., Deutsch, C.V., 2014. A multiple training image approach for spatial modeling of geologic domains. Math. Geosci. 46, 815–840. https://doi.org/10.1007/s11004-014-9543-0, 2014.
Smirnoff, A., Boisvert, E., Paradis, S.J., 2008. Support vector machine for 3D modelling from sparse geological information of various origins. Comput. Geosci. 34 (2), 127–143.
Straubhaar, J., Renard, P., 2021. Conditioning multiple-point statistics simulation to inequality data. Earth Space Sci. 8 (5), e2020EA001515.
Straubhaar, J., Renard, P., Mariethoz, G., Froidevaux, R., Besson, O., 2011. An improved parallel multiple-point algorithm using a list approach. Math. Geosci. 43, 305–328. https://doi.org/10.1007/s11004-011-9328-7.
Strebelle, S., 2002. Conditional simulation of complex geological structures using multiple-point statistics. Math. Geol. 34 (1), 1–21.
Tahmasebi, P., 2018. Multiple point statistics: a review. In: Daya Sagar, B., Cheng, Q., Agterberg, F. (Eds.), Handbook of Mathematical Geosciences. Springer, Cham. https://doi.org/10.1007/978-3-319-78999-6_30.
Tan, X., Tahmasebi, P., Caers, J., 2014. Comparing training-image based algorithms using an analysis of distance. Math. Geosci. 46, 149–169. https://doi.org/10.1007/s11004-013-9482-1.
Toftaker, H., Tjelmeland, H., 2013. Construction of binary multi-grid Markov random field prior models from training images. Math. Geosci. 45, 383–409. https://doi.org/10.1007/s11004-013-9456-3.
Vistelius, A.B., 1989. Principles of Mathematical Geology. Kluwer Academic Publishers, Dordrecht, p. 500.
Zhang, T., Switzer, P., Journel, A., 2006. Filter-based classification of training image patterns for spatial simulation. Math. Geol. 38 (1), 63–80.